Australas Phys Eng Sci Med (2017) 40:675–686
DOI 10.1007/s13246-017-0578-7

SCIENTIFIC PAPER

Estimation of effective brain connectivity with dual Kalman filter and EEG source localization methods

Mehdi Rajabioun[1] · Ali Motie Nasrabadi[2] · Mohammad Bagher Shamsollahi[3]

Received: 16 January 2017 / Accepted: 3 August 2017 / Published online: 29 August 2017

Abstract Effective connectivity is one of the most important considerations in brain functional mapping via EEG. It demonstrates the effects of a particular active brain region on others. In this paper, a new method is proposed which is based on dual Kalman filter. In this method, firstly by using a brain active localization method (standardized low resolution brain electromagnetic tomography) and applying it to EEG signal, active regions are extracted, and appropriate time model (multivariate autoregressive model) is fitted to extracted brain active sources for evaluating the activity and time dependence between sources. Then, dual Kalman filter is used to estimate model parameters or effective connectivity between active regions. The advantage of this method is the estimation of different brain parts activity simultaneously with the calculation of effective connectivity between active regions. By combining dual Kalman filter with brain source localization methods, in addition to the connectivity estimation between parts, source activity is updated during the time. The proposed method performance has been evaluated firstly by applying it to simulated EEG signals with interacting connectivity simulation between active parts. Noisy simulated signals with different signal to noise ratios are used for evaluating method sensitivity to noise and comparing proposed method performance with other methods. Then the method is applied to real signals and the estimation error during a sweeping window is calculated. By comparing proposed method results in different simulation (simulated and real signals), proposed method gives acceptable results with least mean square error in noisy or real conditions.

Keywords Dual Kalman filter · Effective brain connectivity · Source localization methods · Multivariate autoregressive model

✉ Ali Motie Nasrabadi
nasrabadi@shahed.ac.ir

[1] Science and Research Branch, Islamic Azad University, Tehran, Iran

[2] Department of Biomedical Engineering, Faculty of Engineering, Shahed University, Tehran, Iran

[3] Faculty of Electrical Engineering, Sharif University of Technology, Tehran, Iran

Introduction

Most biological systems have several interacting subsystems and an important task in the analysis and study of these systems is to understand how these subsystems are dynamically related to each other and to study the effects of interactions inside the system [1, 2]. Brain is one part of the biological systems with interacting subsystems and its function is associated with interactions between different subsystems and their effects on each other, which has been a challenge in the field of Neuroscience [1–3]. The interaction between brain subsystems is called brain connectivity and its estimation is a subject for calculation and analysis of the direction and amplitude of the data flow among brain areas [1–4]. Three kinds of brain connectivities are proposed for describing such interactions: anatomical or structural connectivity, functional connectivity, and effective connectivity [3]. Anatomical or structural connectivity describes anatomical contact between neural units at a given time and the physical structure of brain is analyzed. It can be calculated using diffusion tensor imaging (DTI) or magnetic resonance imaging (MRI) measuring [5, 6]. Functional connectivity is defined by statistical dependence among neurons of the brain. It can be measured by correlations between neurons in time or frequency domain [7, 8]. Effective connectivity discusses

about how one neural system affects another one. In other words, in effective connectivity, the relations between brain regions or the effects of one region on other regions are analyzed [5, 8–10]. The common difference between functional and effective connectivity is that effective connectivity is described as a driver–receiver relationship [11] or the effect of one region on another region, while functional connectivity is defined as correlation between neurons of the brain [11]. Because of the relations between brain regions and their activities. Hence, understanding the causal relationships between brain activations and effective connectivities between brain neurons are important [12].

Several measures are proposed for evaluating and calculating the brain effective connectivity. These measures can be divided to two large classes; one of which is based on the concept of random variables named data based methods, while the other class is based on fitting specific models on generated data which are called model based methods. The methods for studying effective connectivity are mostly from the second class, such as Granger causality and dynamic causal modeling which are most applicable. In model based method, physiological information is fitted to data [12].

Grange casualty (GC) is one of the models which is based on effective connectivity estimation methods and is based on the supposition that each cause precedes its effects [13]. This method is mostly applied to a linear prediction model such as the multivariate autoregressive (MVAR) model. Directed transfer functions (DTF), partial directed coherence (PDC), and so on are some connectivity measures which are obtainable from this model [3, 13–15]. Dynamic causal model (DCM) can quantify neural connectivity by a bilinear state space model assumption. This framework considers parametric causal and physiological models of the neuronal dynamics. In this method, the model parameters are calculated with certain prior assumptions considerations and model fitting on data. In DCM, the desired variable estimation for effective connectivity is usually not limited to a predetermined network structure [16–18].

The first part in effective connectivity estimation is active source determination and their localization to estimate the connectivity between them. These sources (which are called dipoles) can be positioned by anatomical or physiological information (like DCM) or can be localized by source localization methods. However the, location and strength estimation of brain electrical current source from EEG recording is an ill-posed problem [19]. Hence, several methods are proposed to solve this non-uniqueness. The localization methods use several methodologies to estimate the active dipole location [19]. Some of the methods which are called dipole fitting methods, such as the standard low resolution analysis (sLORETA), minimum norm (MN) or other conventional methods make use of matrix inversion for direct calculation of the active dipoles. Compared with a similar method (i.e. LORETA), sLORETA gives the good and acceptable localization error [19, 20]. Another group of methods such as beamforming, spatial filters are used to estimate brain active sources [21]. Some other methods like independent component analysis (ICA) use model reduction algorithms to remove noise from the EEG signal and dimension reduction by lower order part truncation from decomposition. By independent sources localization, a separate source localization problem is solved. That is, the downhill simplex search method is used for each independent component localization to determine the dipole's components which contribute more in EEG signal forming [21–23].

After sources and their locations extraction, the interaction between sources should be modeled for connectivity estimation. By source interaction modeling and model parameters estimation, the connectivity is calculated from the estimated parameters. The multivariate autoregressive (MVAR) process can provide a model for the temporal effects across different variables (active brain regions and other time series). This model characterizes the relation between regions within the data, specifically in terms of the effect of one variable on another. Several methods have been proposed for multivariate autoregressive (MVAR) parameter estimation [24, 25]. The most traditional methods in this field are Yule–Walker (YW) and modified Yule–Walker (MYW) methods, which are used for estimating correlation AR model delays. From computational point of view, the Yule–Walker method is structurally simple, but it has low estimation, which is a consequence of the use of large-lag autocovariance estimates [25, 26]. Levinson recursion, the Burg-type Nuttall–Strand method, or the Vieira–Morf methods are the other methods in this field that have been known for more than 25 years [27]. Newton–Raphson gradient search method is used for MVAR parameters estimation [28]. Some other methods use maximum likelihood estimation for multivariate AR model identification. Penny and Roberts solved that problem by Bayesian estimation method [29].

By using multivariate autoregressive (MVAR) process, the relations between brain sources can be modeled in the form of linear difference equations [29]. A.H. Omidvarnia used dual Kalman filter for cortical connectivity analysis of newborn EEG in sensor or electrode space [30]. Eduardo Giraldo proposed a new method for a dynamic estimation of neuronal activity and brain dynamics from EEG signals by using dual Kalman filter [31]. In this method, MVAR process is used to model the active source (after source localization and extracting active sources), and dual Kalman Filter is used to calculate the effective connectivity among sources. In the proposed method, source space is used instead of electrode space (which is used by A.H. Omidvarnia [30]). In sensor or electrode space the volume conductor effect or skull and the electrical conductance of other tissues can

influence the EEG recording and disturb electrode readings [19]. In electrode space solution and algorithms the volume conductor effect is ignored [19]. So connectivity estimation from electrode space is not more accurate and valuable than source space. Source space solves this problem by entering volume conductor and tissue conductance effect on lead-field matrix and by solving EEG forward problem [19–23]. The problem of source space is its ill-posedness which is improved by source localization methods [19–23]. In our method the source space is used and dual Kalman filter is applied to estimated active source which is extracted from source localization methods. The main aim of this paper is to propose a method for calculating effective connectivity that is commonly based on dual Kalman filter and source localization combination. Working on source spaces and studying the relation between brain sources helps us to discover valuable information from source interaction between each other in some disorders [19]. By estimating connectivity between active sources, the relation between active regions of brain is calculated. In our method which is based on dual Kalman filter, each state or strength of active source is updated in each run and relations between them are calculated simultaneously. In this study, for comparing new method performance, the proposed method is applied to simulated EEG signals with simulated connectivity and real EEG signals. Then the results are compared with simulated connectivity or other methods for comparison.

The structure of this paper is as follows. The proposed method is introduced and formulated in "Methods" section. It consists of introducing sLORETA as source localization method (which is used in this study), the MVAR model for brain active sources modeling and dual Kalman filter formulations (a method for estimating unknown model parameters). "Data synthesis and validation methods" section discusses the study simulations, the signal generations with known and predefined connectivity and real EEG signals for connectivity estimation by proposed method. The results of simulations and applying proposed method to simulated or real signals is discussed in "Model implementation and result" section. Some other methods are used for comparing method performance with other methods in "Model implementation and result" section. In the last section, the conclusions of applying proposed method to EEG signals and their results are discussed.

Methods

The method proposed by this study is based on dual Kalman filter and source localization method and is used for estimating effective connectivity of brain active regions. An illustration and diagram of proposed method is presented in Fig. 1.

Before connectivity estimation, it is necessary to apply a source localization method to EEG signals which is recorded by electrodes and brain source temporal signals are estimated by leadfield matrix and EEG signals. This method is made of three steps. In the first step, static or dynamic source localization of the active brain sources is done. This stage is only used for determining active dipoles because of complexity reduction.

The output of this level is the limited number of active dipoles (it must be less than channel numbers because of dual Kalman filter limitation) with their positions. In this step the goal is to minimize the following function:

$$\boldsymbol{F} = \|\boldsymbol{V}_k - \boldsymbol{G}\boldsymbol{J}_k\|_2 + \alpha\|\boldsymbol{J}_k\|_2 \tag{1}$$

where $\boldsymbol{V}_k(m \times 1)$ is EEG signal at instant k, $\boldsymbol{G}(m \times n)$ is leadfield matrix which is calculated from forward problem solution [19, 32–34], $\boldsymbol{J}_k(n \times 1)$ is dipole or source vector at instant k, m is the number of EEG channels, n is the number of brain dipoles and α is regularization parameter and controls the source activity contribution to estimation error and cost function (Eq. 1). The regularization parameter is used for decreasing the sensitivity of localization method to noise and is determined by regularization methods like Tikhonov or l-curve [19]. This function is to be minimized with respect to $\boldsymbol{J}_k$, for given $\mathbf{G}$, $\boldsymbol{V}_k$, and α. The explicit solution to this minimization problem in sLORETA is [19, 20]:

$$\hat{\boldsymbol{J}}_k = \boldsymbol{T} \cdot \boldsymbol{V}_k \tag{2}$$

where $\hat{\boldsymbol{J}}_k$ is the estimated dipole activation matrix

$$\boldsymbol{T} = \boldsymbol{G}^T\boldsymbol{H}\left[\boldsymbol{H}\boldsymbol{G}\boldsymbol{G}^T\boldsymbol{H} + \alpha\boldsymbol{H}\right]^+ \tag{3}$$

$$\boldsymbol{H} = \boldsymbol{I} - 11^T/1^T1 \tag{4}$$

where $[\cdot]^+$ is pseudoinverse of matrix, and in our method α is calculated by Tikhonov regularization method and is set to 0.1.

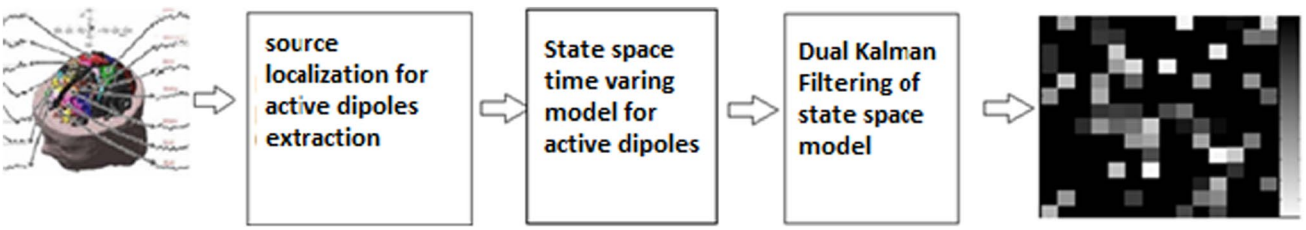

Fig. 1 Illustration of proposed method

After estimation of dipole vector ($\hat{\boldsymbol{J}}_{\boldsymbol{k}}$) during the signal recording time, the dipoles which are active during the time are extracted as active dipoles. Clearly the dipoles which have more chance to be selected during the recoding time are selected as final active dipoles.

After active dipole extraction in the second step, a linear dynamic model is assumed as follows for active dipoles:

$$\boldsymbol{J}_{\boldsymbol{k}} = \boldsymbol{F}_{\boldsymbol{k}}\boldsymbol{J}_{k-1} + \eta_k \tag{5}$$

where $\boldsymbol{J}_{\boldsymbol{k}}$ is a vector with $(n \times 1)$ and η_k is state noise. Hence, EEG signal can be written by leadfield matrix which is simplified with extracted active dipoles as follows:

$$\boldsymbol{V}_{\boldsymbol{k}} = \boldsymbol{G}\boldsymbol{J}_{\boldsymbol{k}} + \varepsilon_k \tag{6}$$

Therefore, the linear and discrete form of this model is a discrete state space system:

$$\begin{aligned} \boldsymbol{J}_{k+1} &= \boldsymbol{F}_{\boldsymbol{k}}\boldsymbol{J}_{\boldsymbol{k}} + \eta_k \\ \boldsymbol{V}_{\boldsymbol{k}} &= \boldsymbol{G}\boldsymbol{J}_{\boldsymbol{k}} + \varepsilon_k \end{aligned} \tag{7}$$

where ε_k, η_k are additive measurement and state noise respectively. The state or process noise (η_k) is the noise in state equation or first expression of Eq. 7. The measurement noise ε_k which is shown in second expression of Eq. 7 is the noise of measurement equipment and so on. These noise covariance matrixes are defined as follows:

$$\begin{cases} \boldsymbol{R}_{\boldsymbol{\eta}} = E\{\eta_k \hat{\eta}_k\} \\ \boldsymbol{R}_{\boldsymbol{e}} = E\{\varepsilon_k \hat{\varepsilon}_k\} \end{cases} \tag{8}$$

If $\boldsymbol{F}_{\boldsymbol{k}}$ and $\boldsymbol{G}$ are known in Eq. 7, $\boldsymbol{J}_{\boldsymbol{k}}$ can be estimated from observation $\boldsymbol{V}_{\boldsymbol{k}}$ by ordinary Kalman filter (KF). But in this model $\boldsymbol{F}_{\boldsymbol{k}}$ is unknown hence $\boldsymbol{J}_{\boldsymbol{k}}$ and $\boldsymbol{F}_{\boldsymbol{k}}$ should be estimated simultaneously by dual Kalman filter (DKF).

In general, the dual Kalman filter process is classified to the modeling, estimation, and prediction parts. In this study, the modeling task is used for approximating the process of dynamics which can be generated from the states in noisy observations. Dual estimation methods use the model for signal estimation and the signal for model parameters estimation.

At each step, a KF(called state KF) is used for state estimation by the current model $\hat{\boldsymbol{F}}_{\boldsymbol{k}}$ calculation, while another KF(called weight KF) is applied for weight calculation by current state $\hat{\boldsymbol{J}}_{\boldsymbol{k}}$ estimation. This process is schematically shown in Fig. 2.

In dual Kalman filter, two ordinary Kalman filters are used which are working in parallel with each other. The top KF is used for state estimation and the bottom one is for model weights calculations. Before dual Kalman Filter formulation, a simple dynamic model should be assumed for $\boldsymbol{F}_{\boldsymbol{k}}$:

$$\begin{cases} \boldsymbol{F}_{\boldsymbol{k}} = \boldsymbol{F}_{k-1} + u_{1k} \\ \boldsymbol{J}_{\boldsymbol{k}} = \boldsymbol{C}_{\boldsymbol{k}}\boldsymbol{F}_{\boldsymbol{k}} + u_{2k} \end{cases} \tag{9}$$

With the covariance of process noise matrix which is defined as:

$$\begin{cases} \boldsymbol{R}_{\boldsymbol{u}1} = E\{u_{1k}{u_{1k}}^T\} \\ \boldsymbol{R}_{\boldsymbol{u}2} = E\{u_{2k}{u_{2k}}^T\} \end{cases} \tag{10}$$

where u_{1k} and u_{2k} are the process and measurement noise of Eq. 9 and $\boldsymbol{C}_{\boldsymbol{k}}$ is defined as:

$$C_k = \begin{bmatrix} \boldsymbol{J}_1^{(k-1)} & \cdots & \boldsymbol{J}_{\boldsymbol{m}}^{(k-1)} & 0 & \cdots & 0 \\ 0 & \boldsymbol{J}_1^{(k-1)} & \cdots & \boldsymbol{J}_{\boldsymbol{m}}^{(k-1)} & 0 & \cdots \\ & \vdots & & & \ddots & \vdots \\ & 0 \ \ldots \ 0 & & & \cdots & \boldsymbol{J}_1^{(k-1)} \ \ldots \ \boldsymbol{J}_{\boldsymbol{m}}^{(k-1)} \end{bmatrix} \tag{11}$$

Then the dual KF equations are presented as follows:

1. Initialization

$$\boldsymbol{P}_{\boldsymbol{F}_0} = E\left[(\boldsymbol{F} - E[\boldsymbol{F}])(\boldsymbol{F} - E[\boldsymbol{F}])^T\right] \tag{12}$$

$$\boldsymbol{P}_{\boldsymbol{J}_0} = E\left[(\boldsymbol{J} - E[\boldsymbol{J}])(\boldsymbol{J} - E[\boldsymbol{J}])^T\right] \tag{13}$$

2. For each sample of time ($k \in \{1, \ldots, T\}$), the time-updates equation

$$\hat{\boldsymbol{F}}_{\bar{\boldsymbol{k}}} = \hat{\boldsymbol{F}}_{\boldsymbol{k}-1} \tag{14}$$

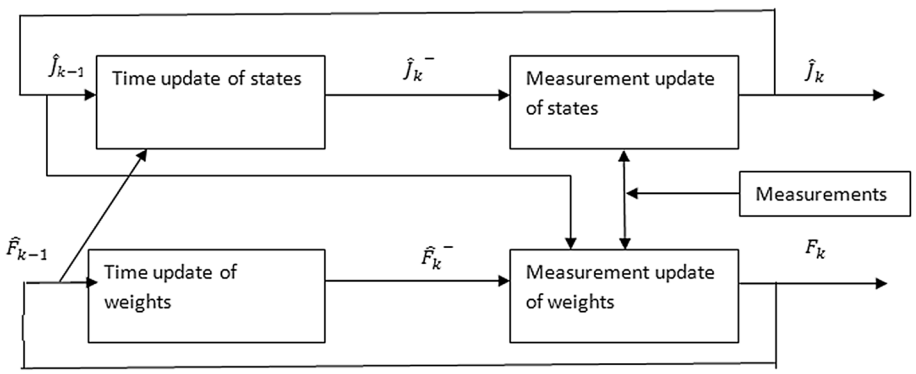

Fig. 2 The dual Kalman filter algorithm

$$\boldsymbol{P}_{\bar{F}_k} = \boldsymbol{P}_{F_{k-1}} + \boldsymbol{R}_{u1} = \lambda^{-1}\boldsymbol{P}_{F_{k-1}} \tag{15}$$

where $\boldsymbol{R}_{u1}$ is the covariance of process noise at k − 1 time sample.

3. The state filter is calculated as follows:

$$\hat{\boldsymbol{J}}_{\bar{k}} = \hat{\boldsymbol{F}}_K \hat{\boldsymbol{J}}_{K-1} \tag{16}$$

$$\boldsymbol{P}_{\bar{J}_k} = \hat{\boldsymbol{F}}_K \boldsymbol{P}_{J_{k-1}} \hat{\boldsymbol{F}}_K^T + \boldsymbol{R}_\eta \tag{17}$$

where $\boldsymbol{R}_\eta$ is covariance of state noise.

4. The measurement update equation is

$$\boldsymbol{K}_k^J = \boldsymbol{P}_{\bar{J}_k} \boldsymbol{G}^T \left(\boldsymbol{G}\boldsymbol{P}_{\bar{J}_k} \boldsymbol{G}^T + \boldsymbol{R}_e \right)^{-1} \tag{18}$$

$$\hat{\boldsymbol{J}}_k = \hat{\boldsymbol{J}}_{\bar{k}} + \boldsymbol{K}_k^J \left(\boldsymbol{V}_k - \boldsymbol{G}\hat{\boldsymbol{J}}_{\bar{k}} \right) \tag{19}$$

$$\boldsymbol{P}_{J_k} = (\boldsymbol{I} - \boldsymbol{K}_k^J \boldsymbol{G}) \boldsymbol{P}_{\bar{J}_k} \tag{20}$$

where $\boldsymbol{R}_e$ is covariance of measurement noise.

5. And for the weight filter

$$\boldsymbol{K}_k^F = \boldsymbol{P}_{\bar{F}_k} \boldsymbol{C}_k^T \left(\boldsymbol{C}_k \boldsymbol{P}_{\bar{F}_k} \boldsymbol{C}_k^T + \boldsymbol{R}_{u2} \right)^{-1} \tag{21}$$

$$\hat{\boldsymbol{F}}_k = \hat{\boldsymbol{F}}_{\bar{k}} + \boldsymbol{K}_k^F \left(\hat{\boldsymbol{J}}_k - \boldsymbol{G}\hat{\boldsymbol{F}}_{\bar{k}} \right) \tag{22}$$

$$\boldsymbol{P}_{F_k} = (\boldsymbol{I} - \boldsymbol{k}_k^F \boldsymbol{C}_k) \boldsymbol{P}_{\bar{F}_k} \tag{23}$$

For clarification, the equations are specified for white-noise case. In dual Kalman filter, the equations must be linearized by recurrent derivatives which are similar to real-time recurrent learning [35].

For a better description of $\boldsymbol{F}$, the first part of state space equation is rewritten as follows:

$$\begin{bmatrix} J_1(n+1) \\ \vdots \\ J_d(n+1) \end{bmatrix} = \begin{bmatrix} F_{11} & \cdots & F_{1d} \\ \vdots & \ddots & \vdots \\ F_{d1} & \cdots & F_{dd} \end{bmatrix} \begin{bmatrix} J_1(n) \\ \vdots \\ J_d(n) \end{bmatrix} \tag{24}$$

The parameter F_{ij} reflects effective relation between ith source at nth time sample to jth source in (n + 1)th time sample. When $\boldsymbol{F}$ is determined, effective connectivity between sources can be represented.

Data synthesis and validation methods

In this study, firstly, the proposed method is applied to simulated EEG signals for validation of the results. These signals are generated by assuming some active dipoles with simulated connectivity between them. In order to simulate the method, four dipoles have been selected for EEG signal generation and these dipoles are shown in Fig. 3.

In the first simulation the connectivity is fixed during the time. The relations between these dipoles are assumed as follows [30]:

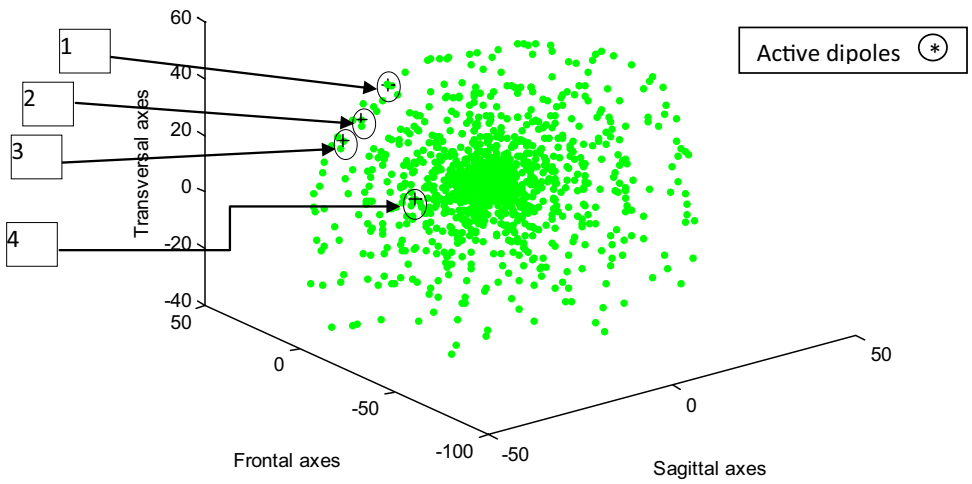

Fig. 3 The four active dipoles used for simulations. The relations is defined between these sources and EEG signal is generated

$$\left.\begin{aligned} \boldsymbol{J}_1(n) &= 0.65\boldsymbol{J}_1(n-1) + a(n)\boldsymbol{J}_2(n-1) + b(n)\boldsymbol{J}_3(n-1) + \eta_1(n) \\ \boldsymbol{J}_2(n) &= 0.87\boldsymbol{J}_2(n-1) + c(n)\boldsymbol{J}_3(n-1) + \eta_2(n) \\ \boldsymbol{J}_3(n) &= 0.56\boldsymbol{J}_3(n-1) + \eta_3(n) \\ \boldsymbol{J}_4(n) &= 0.87\boldsymbol{J}_4(n-1) + \eta_4(n) \\ \boldsymbol{J}_l(n) &= \eta_l(n) \quad l = 5 \ldots 19 \text{ (for other dipoles)} \end{aligned}\right\} \tag{25}$$

$$\boldsymbol{J}_1(1) = \boldsymbol{J}_2(1) = \boldsymbol{J}_3(1) = \boldsymbol{J}_4(1) = 1$$

where $J_i(n)$ is the ith dipole activation in nth sample. In this simulation, a(n), b(n), c(n) are set fixed during the time and have the values of 0.9, 0.5, 0.7 respectively. These parameters are the known relations between these four dipoles, which is called effective connectivity.

After generating dipole's activation value in the time samples ($\boldsymbol{J_i}$), EEG signal is generated by multiplying dipole's activation values by leadfield matrix which is calculated by FEM or BEM methods [32, 36, 37]. In our work this matrix is calculated with fieldtrip toolbox of MATLAB software.

$$\boldsymbol{V}(n) = \boldsymbol{G}\boldsymbol{J}(n) + \boldsymbol{\epsilon} \tag{26}$$

where $\boldsymbol{G}$ is leadfield matrix and ϵ is measurement noise. After generating the simulated signal the proposed method is applied to the generated signal ($V(n)$). The source localization method which is used in our simulations is Standardized low resolution brain electromagnetic tomography (sLORETA) [38]. As discussed earlier, sLORETA gives good localization error in comparison with other methods which makes use of matrix inversion to localize the active dipoles. Then, active dipoles from all of the samples are extracted and state space model (Eq. 5) is fit into the extracted dipoles. Finally, dual Kalman filter is applied to the model to estimate $\boldsymbol{F}$ and $\boldsymbol{J}$. In this simulation $\boldsymbol{F}$ is estimated connectivity and $\boldsymbol{J}$ is estimated dipole activation in the sample; the connectivity between dipoles is assumed to be constant in time.

In the second simulation, the connectivity estimation is done in different levels of noisy signals such that the noise is added to signal with different signal to noise ratios (SNRs) and the method performance in connectivity estimation to these noisy signals is studied. In state space model, two different noise exist, state noise (η) and measurement noise (ϵ). Furthermore, the simulated connectivities between dipoles are fixed during the time and their values are the same as the connectivity values of first simulation.

Most of the brain connectivities are not fixed during time. So the connectivity between active dipoles must be assumed to be varied during the time. The third simulation is done for estimating time varying connectivities between dipoles which are assumed to be varied during the time and the method is applied to EEG signals which are simulated with time-varying connectivity. The time varying connectivities are shown in Fig. 4 which shows the value of connectivity parameters versus time. After active dipole simulations, the EEG signal is generated as discussed above (Eq. 26). The mean square error of the difference between estimated and known error is calculated with different methods for

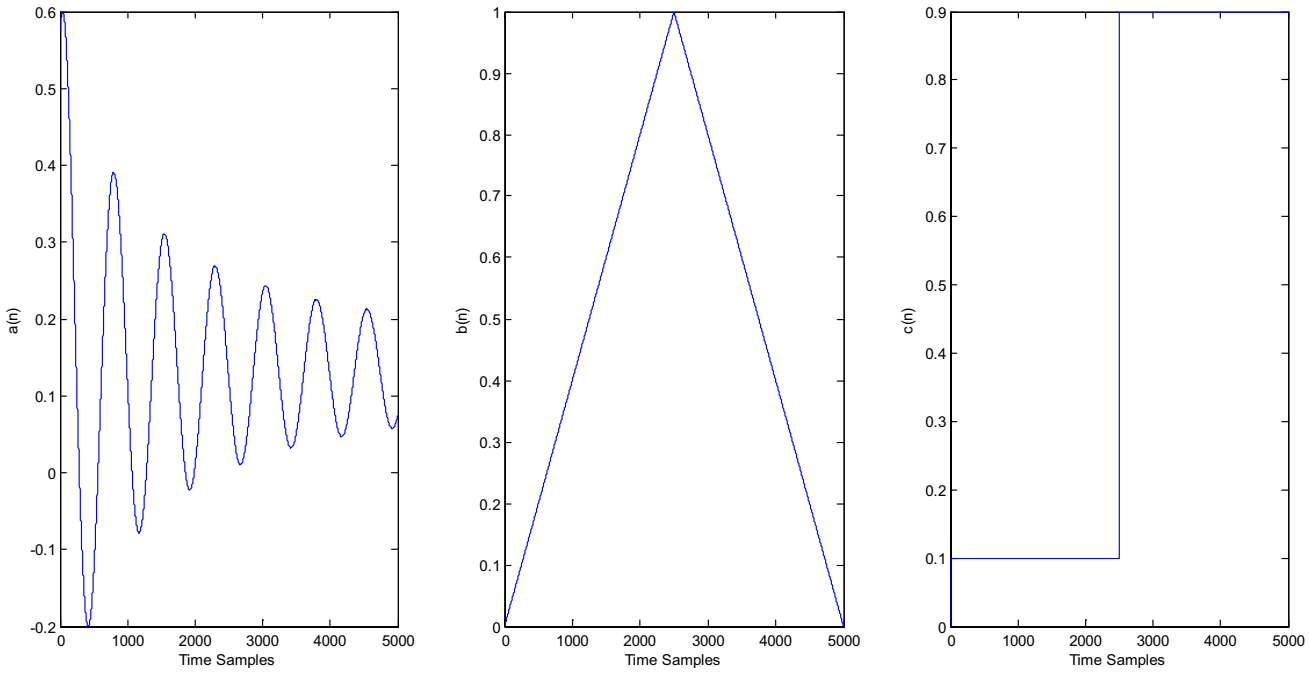

Fig. 4 Plots of a(n), b(n) and c(n) versus samples of time which are defined in Eq. 25. These parameters (as defined in Eq. 25) are assumed between dipoles to simulate EEG signals

comparing proposed method performance. The other methods which are used for comparison are MVAR parameter estimations and EEG signals should be changed to source activity which is done by matrix inversion of leadfield. In the last part of this simulation the estimated connectivities which are calculated by proposed method are plotted versus samples of time for method validation.

In the fourth simulation, the ability of the method to estimate the connectivity with higher model order is studied in which the degree of model or the state equation is set second order of MVAR model. As demonstrated in Eq. 25, the model order of the previous simulation is one and in this simulation the method performance to estimate the connectivity with higher order model is analyzed. The formulation of this part is as follows:

$$\left.\begin{aligned} \boldsymbol{J}_1(n) &= 0.65\boldsymbol{J}_1(n-1) + a(n)\boldsymbol{J}_2(n-2) + \boldsymbol{b(n)}\boldsymbol{J}_3(n-1) + \eta_1(n) \\ \boldsymbol{J}_2(n) &= 0.87\boldsymbol{J}_2(n-1) + c(n)\boldsymbol{J}_3(n-1) + \eta_2(n) \\ \boldsymbol{J}_3(n) &= 0.56\boldsymbol{J}_3(n-1) + \eta_3(n) \\ \boldsymbol{J}_4(n) &= 0.87\boldsymbol{J}_4(n-1) + \eta_4(n) \\ \boldsymbol{J}_l(n) &= \eta_l(n) \quad l = 5 \ldots 19 \text{ (for other dipoles)} \end{aligned}\right\} \tag{27}$$

$$\boldsymbol{J}_1(1) = \boldsymbol{J}_2(1) = \boldsymbol{J}_3(1) = \boldsymbol{J}_4(1) = 1$$

In the last simulation, the real data is used for method validation. These data are recorded from normal children at HRL laboratories and UCLA Semel Institute for Neuroscience and Human behavior with open eyes and fixed on a spot directly in front of them. In preprocessing step, a high pass filter with 1 Hz cutoff frequency is applied to signal for baseline drift and low variation removing. A sweeping window is defined which moves along the signal and model parameters are estimated inside the window by proposed method. Then, the last sample of window is reconstructed by model parameters and compared with real sample of signal. The mean square error between real and reconstructed sample of each window during the signal is calculated. In this simulation three example signals are used for this simulation.

Model implementation and result

After data synthesis and defining validation methods, the proposed method should be applied to these data. The proposed method algorithm is shown in Fig. 5.

In the first simulation the connectivity among dipoles during the time are set fixed. In the first simulation the connectivity [a(n), b(n) and c(n) in Eq. 25] are assumed to be fixed and with the values of 0.5, 0.9 and 0.7 respectively. After EEG simulations with underlying interacting connectivity are done, the source localization method is applied on signals during the time and more active diploes of each time are estimated. The dipoles which are more active during the time are extracted and active dipoles of this simulation are plotted in Fig. 6.

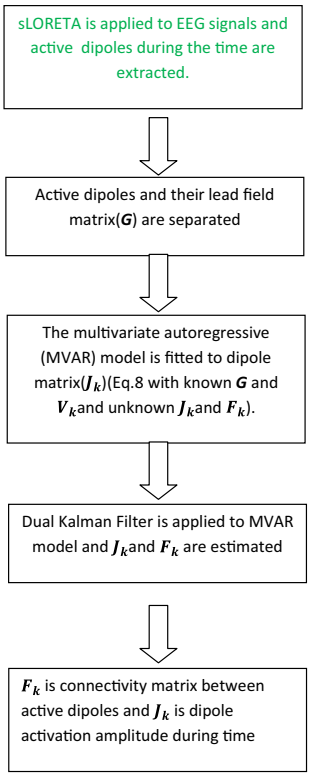

Fig. 5 The flowchart of proposed method steps

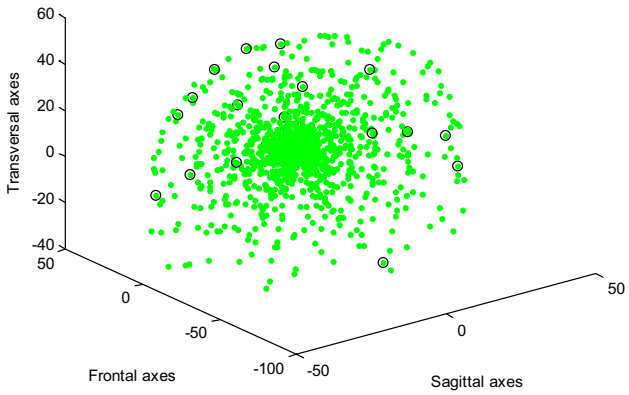

Fig. 6 The estimated active diploes plotted in source space. These dipoles are recognized to be active by sLORETA localization algorithm in the first stage

Then dual Kalman filter is applied to signals and estimated connectivity matrix is calculated. The mean of extracted connectivity during the time is the feature to separate simulated dipoles. The connectivity of simulated dipoles is shown in Fig. 7. It can be concluded that the estimated

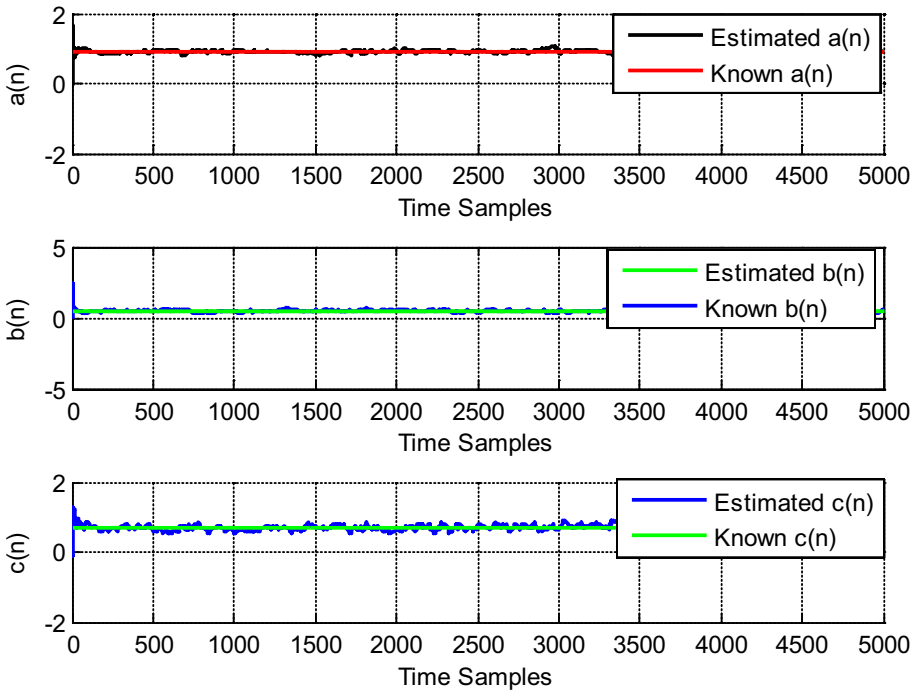

Fig. 7 Plot of the estimated a(n), b(n) and c(n) with known connectivity against time samples

Table 1 The mean and mean square error of estimated time invariant connectivity in several state noise levels

SNR in dB	Actual value	Estimated value			
		−10	0	10	20
Mean					
a(n)	0.9	0.8996	0.8956	0.8960	0.9979
b(n)	0.5	0.4831	0.4676	0.4821	1.4519
c(n)	0.7	0.7072	0.7038	0.7128	0.5038
Mean square error					
a(n)		0.0552	0.0542	0.0725	1.9939
b(n)		0.0865	0.0922	0.0794	3.5356
c(n)		0.1140	0.0768	0.1097	0.6376

Table 2 The mean and mean square error of estimated time invariant connectivity in several measurement noise levels

SNR in dB	Actual value	Estimated value			
		10	20	30	40
Mean					
a(n)	0.9	0.6846	0.8453	0.8832	0.9103
b(n)	0.5	0.3291	0.4678	0.5110	0.4933
c(n)	0.7	0.5453	0.6734	0.7167	0.7043
Mean square error					
a(n)		1.0760	0.1022	0.0389	0.0134
b(n)		0.5851	0.0828	0.0674	0.0120
c(n)		1.0110	0.0826	0.0895	0.0150

connectivity gives acceptable answers in comparison with simulated connectivity. The mean of estimated connectivity (0.8996, 0.4831 and 0.7072) is close to the underlying interacting connectivity which is set active in signal simulation step.

In the second simulation, the performance of proposed method in noisy environment is analyzed since the connectivity of dipoles is the same as the first simulation. The results of applying proposed method to noisy EEG signals are reported in Tables 1 and 2.

In Table 2, the mean and mean square error of estimated connectivity are shown in different measurement noise (in Eq. 7) levels. The results of this table show that a good estimate was found for SNRs more than 20 dB (Table 3).

Table 1 shows the mean and mean square error of estimated time invariant connectivity with state noise (η_k in Eq. 7) variation. It can be concluded from Table 1 that the method gives a better and closer result by decreasing signal to noise ratio of state noise. It can be concluded that by increasing state noise or decreasing SNR the mean value gets closer to actual values and its mean square error decreases. On the other hand, Table 2 shows that by increasing measurement noise level or decreasing SNR the mean value of signal becomes far from actual value and mean square error of signal increases.

In the third simulation, the connectivity among active dipoles is assumed to be varied through the time according to what occurs in real brain. The time varying functions are shown in Fig. 4. After EEG generation and applying

Table 3 The mean square error of different methods in estimating connectivities of Eq. 25

SNR in dB	10	20	30	40
Proposed method				
a(n)	1.0523	0.1835	0.0893	0.0861
b(n)	1.9943	0.2237	0.1031	0.0904
c(n)	1.5700	0.1762	0.1249	0.1116
Method 1				
a(n)	2.2439	0.1283	0.0652	0.0192
b(n)	2.9124	0.1752	0.0824	0.0264
c(n)	2.4435	0.1462	0.0459	0.0265
Method 2				
a(n)	1.9923	0.1023	0.0541	0.0184
b(n)	2.4023	0.1932	0.0851	0.0293
c(n)	2.2787	0.0943	0.0591	0.0398
Method 3				
a(n)	2.5321	0.1325	0.0425	0.0152
b(n)	3.1362	0.1653	0.0616	0.0291
c(n)	3.0235	0.1042	0.0449	0.0352

proposed method to simulated signal, the estimated connectivity matrix is calculated.

For comparing proposed method in this study, several other methods are applied to generated signals with different SNRs of measurement noise. In other comparative methods leadfield matrix is calculated by forward problem and inverted and then applied to generated EEG signals. Then EEG signals are converted to source space activities and three methods are applied to source activities for connectivity estimation. The mean square error of the difference between estimated connectivity and known connectivities which are calculated by different methods are shown in Table 3. The other methods which are used in this simulation are as follows:

- Method 1: modified Yule–Walker [25]
- Method 2: Newton–Raphson gradient search method [28]
- Method 3: Vieira–Morf [27]

As it can be concluded from Table 3, the proposed method gives better error in comparison with other related methods. The estimated connectivities have some variations close to simulated connectivities and proposed method gives less MSE than other methods. It is because of the advantage of proposed method which the connectivity estimation is done in parallel with active source localization method. But in other methods, first, source localization method is applied to signal and source activities are not updated during the signal.

After applying connectivity matrix estimation, meaningful connectivities are extracted and plotted in Figs. 8, 9 and 10. As it can be concluded from these figures, the proposed method gives an acceptable and good result in comparison with simulated connectivity functions.

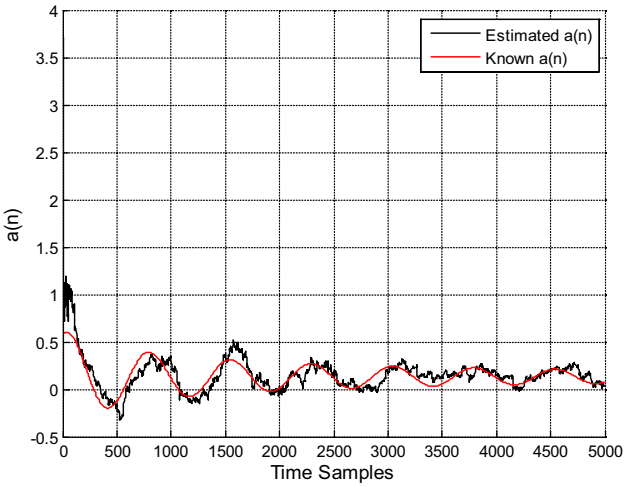

Fig. 8 Plot of the estimated a(n) (which is defined in Eq. 25) and known connectivity against time samples

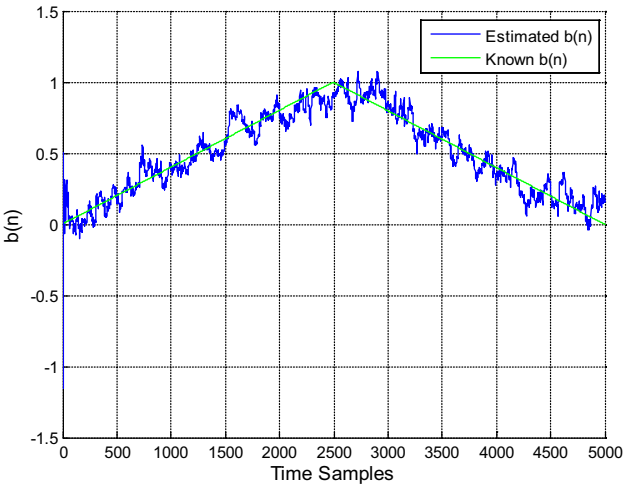

Fig. 9 Plot of the estimated b(n) (which is defined in Eq. 25) and known connectivity against time samples

The fourth simulation is for estimating the connectivity which is defined by second order of MVAR model. In this step, the result of applying proposed method to signals is analyzed when they are generated from second order connectivity (defined by second order MVAR model which is shown in Eq. 27). The estimated connectivity [a(n)] and underlying simulated version are shown in Fig. 11.

As can be deduced from the figure, the method proposed in this study gives an acceptable estimation of the connectivity among dipoles (not as good as first order model) as the model order increases. By comparing Figs. 8 and 11, it can be concluded that the proposed method can estimate higher

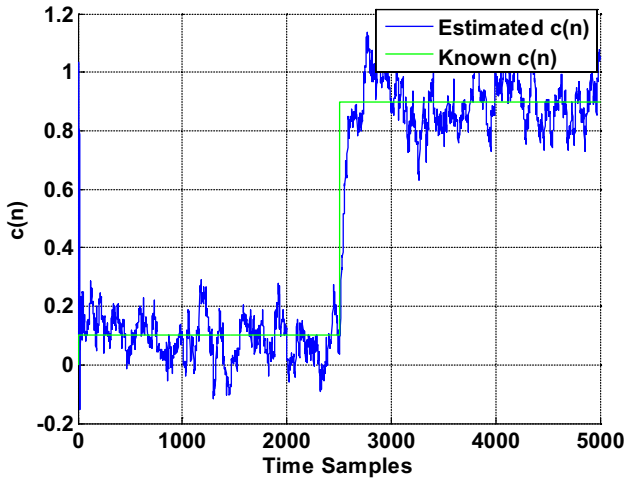

Fig. 10 Plot of the estimated c(n) (which is defined in Eq. 25) and known connectivity against time samples

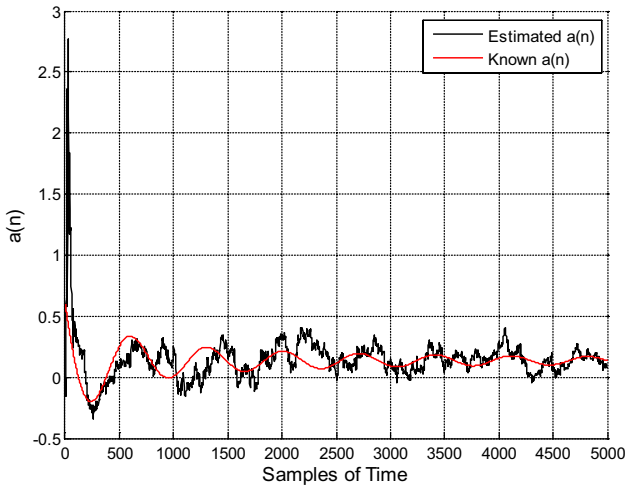

Fig. 11 Plot of the estimated higher order connectivity a(n) (which is defined in Eq. 27) and simulated connectivity against time samples

order connectivity. In Fig. 8 the order of connectivity or the order of model which defines the connectivity with that model is one (Eq. 25) and in Fig. 11 the defined model order for connectivity is two (Eq. 27). The proposed method can estimate both of them (Eqs. 25 and 27) correctly and it can be used for estimating higher order model for connectivity definition.

The last simulation is done on real EEG sample signals of three normal children. These signals have the amplitude about 30 μV. A sweeping window with the length of 64 samples is moved 32 samples in each run during the signal. Then the connectivity between two sample dipoles is estimated inside the window and the model parameters are calculated in moving window. The last sample of window is reconstructed from estimated parameters and is compared with real value of that sample. The mean square error of all windows of signals and the result of this error are in Table 4. As it can concluded from Table 4, the proposed method gives accurate and acceptable mean square error in three signals.

Table 4 The mean square error between reconstructed and real sample of EEG signal for reconstructing last sample of sweeping window

	Signal no. 1	Signal no. 2	Signal no. 3
Mean square error	0.2338	0.0567	0.0709

Conclusion

Studying the relations and interactions among brain regions and its functional workings is one of the important fields in analyzing brain function. These relations which are called brain connectivity are divided into 3 fields. One of the connectivity subsections is effective connectivity. The proposed method in this paper is used for estimating effective connectivity of brain by dual Kalman filter. Dual Kalman filters are used in prediction and estimation of states and the relation between states simultaneously from observations. It is used when state space model is assumed between states and observations when states and their relations are unknown. In this paper Dual Kalman filter is used for estimating the brain regions activity and their relations by considering EEG signals as observations. The proposed method estimates connectivity in conjunction with dynamic source activation detection and its modification. So it is more accurate than other methods which use static source activation algorithms. This method does not need any predefined information (such as other model based methods). In this paper, first, simulated and generated signal is used for method validation whose connectivities are known and signal is generated from known connectivity. As it can be understood from the results, the proposed method gives acceptable and reliable results in estimating time-varying and time-invariant connectivities with different model orders. The results of proposed method to noisy data in several levels are analyzed. The proposed method can be used for connectivity estimation when higher order model is used for connectivity modeling. The performance of method is compared with other methods in estimating time varying connectivity and the results show that the proposed method because of simultaneous estimation of source activities gives a better result than other methods. Lastly, the method is applied to three real EEG signals and their estimation error during sweeping window is analyzed. In future works, this method can be applied to other EEG

signals to estimate effective connectivity of brain which can be used for analyzing neurological disorders such as Autism.

Acknowledgements This research has been supported by Cognitive Science and Technologies Council, Iran.

Compliance with ethical standards

Conflict of interest The authors declare that they have no conflict of interest.

Ethical approval This article does not contain any studies with human participants or animals performed by any of the authors.

References

1. Li Y, Tang X, Xu Z, Liu W, Li J (2016) Temporal correlation between two channels EEG of bipolar lead in the head midline is associated with sleep-wake stages. Australas Phys Eng Sci Med 39(1):147–155. doi:10.1007/s13246-015-0409-7
2. Berry T, Hamilton F, Peixoto N, Sauer T (2012) Detecting connectivity changes in neuronal networks. J Neurosci Methods 209(2):388–397. doi:10.1016/j.jneumeth.2012.06.021
3. Sakkalis V Review of advanced techniques for the estimation of brain connectivity measured with EEG/MEG. Comput Biol Med 41 (12):1110–1117. doi:10.1016/j.compbiomed.2011.06.020
4. Greenblatt RE, Pflieger ME, Ossadtchi AE (2012) Connectivity measures applied to human brain electrophysiological data. J Neurosci Methods 207(1):1–16. doi:10.1016/j.jneumeth.2012.02.025
5. Sargolzaei S, Cabrerizo M, Goryawala M, Eddin AS, Adjouadi M Scalp EEG brain functional connectivity networks in pediatric epilepsy. Comput Biol Med 56:158–166. doi:10.1016/j.compbiomed.2014.10.018
6. Billinger M, Brunner C, Müller-Putz GR (2015) Online visualization of brain connectivity. J Neurosci Methods 256:106–116. doi:10.1016/j.jneumeth.2015.08.031
7. Ahmad RF, Malik AS, Kamel N, Reza F, Abdullah JM (2016) Simultaneous EEG-fMRI for working memory of the human brain. Australas Phys Eng Sci Med 39(2):363–378. doi:10.1007/s13246-016-0438-x
8. Khadem A, Hossein-Zadeh G-A (2014) Estimation of direct nonlinear effective connectivity using information theory and multilayer perceptron. J Neurosci Methods 229:53–67. doi:10.1016/j.jneumeth.2014.04.008
9. Plis SM, Weisend MP, Damaraju E, Eichele T, Mayer A, Clark VP, Lane T, Calhoun VD Effective connectivity analysis of fMRI and MEG data collected under identical paradigms. Comput Biol Med 41 (12):1156–1165. doi:10.1016/j.compbiomed.2011.04.011
10. Vicente R, Wibral M, Lindner M, Pipa G (2011) Transfer entropy–a model-free measure of effective connectivity for the neurosciences. J Comput Neurosci 30(1):45–67. doi:10.1007/s10827-010-0262-3
11. Haufe S (2012) Towards EEG source connectivity analysis. Berlin University of Technology, Berlin
12. Florin E, Pfeifer J Statistical pitfalls in the comparison of multivariate causality measures for effective causality. Comput Biol Med 43(2):131–134. doi:10.1016/j.compbiomed.2012.11.009
13. Pyka M, Heider D, Hauke S, Kircher T, Jansen A (2011) Dynamic causal modeling with genetic algorithms. J Neurosci Methods 194(2):402–406. doi:10.1016/j.jneumeth.2010.11.007
14. Sakkalis V, Giurc CD, Xanthopoulos P, Zervakis ME, Tsiaras V, Yang Y, Karakonstantaki E, Micheloyannis S (2009) Assessment of linear and nonlinear synchronization measures for analyzing EEG in a mild epileptic paradigm. IEEE Trans Inf Technol Biomed 13(4):433–441. doi:10.1109/TITB.2008.923141
15. Barnett L, Seth AK (2014) The MVGC multivariate Granger causality toolbox: a new approach to Granger-causal inference. J Neurosci Methods 223:50–68. doi:10.1016/j.jneumeth.2013.10.018
16. Aponte EA, Raman S, Sengupta B, Penny WD, Stephan KE, Heinzle J (2016) mpdcm: a toolbox for massively parallel dynamic causal modeling. J Neurosci Methods 257:7–16. doi:10.1016/j.jneumeth.2015.09.009
17. Penny WD, Litvak V, Fuentemilla L, Duzel E, Friston K (2009) Dynamic causal models for phase coupling. J Neurosci Methods 183(1):19–30. doi:10.1016/j.jneumeth.2009.06.029
18. Ibrahim RA (1993) Engineering applications of correlation and spectral analysis—Julius S. Bendat and Allan G. Piersol. AIAA Journal 31(11):2190–2191. doi:10.2514/3.49131
19. Grech R, Cassar T, Muscat J, Camilleri KP, Fabri SG, Zervakis M, Xanthopoulos P, Sakkalis V, Vanrumste B (2008) Review on solving the inverse problem in EEG source analysis. J NeuroEng Rehabil 5(1):25. doi:10.1186/1743-0003-5-25
20. Jatoi MA, Kamel N, Malik AS, Faye I (2014) EEG based brain source localization comparison of sLORETA and eLORETA. Australas Phys Eng Sci Med 37(4):713–721. doi:10.1007/s13246-014-0308-3
21. Jonmohamadi Y, Poudel G, Innes C, Jones R (2014) Source-space ICA for EEG source separation, localization, and time-course reconstruction. Neuroimage 101:720–737. doi:10.1016/j.neuroimage.2014.07.052
22. Brookings T, Ortigue S, Grafton S, Carlson J (2009) Using ICA and realistic BOLD models to obtain joint EEG/fMRI solutions to the problem of source localization. Neuroimage 44(2):411–420. doi:10.1016/j.neuroimage.2008.08.043
23. Jonmohamadi Y, Poudel G, Innes C, Jones R (2014) Voxel-ICA for reconstruction of source signal time-series and orientation in EEG and MEG. Australas Phys Eng Sci Med 37(2):457–464. doi:10.1007/s13246-014-0265-x
24. Harrison L, Penny WD, Friston K (2003) Multivariate autoregressive modeling of fMRI time series. Neuroimage 19(4):1477–1491. doi:10.1016/S1053-8119(03)00160-5
25. Mahmoudi A, Karimi M (2008) Estimation of the parameters of multichannel autoregressive signals from noisy observations. Signal Process 88(11):2777–2783. doi:10.1016/j.sigpro.2008.06.004
26. Xing WZ (2000) Autoregressive parameter estimation from noisy data. IEEE Trans Circuits Syst II 47(1):71–75. doi:10.1109/82.818897
27. Schlögl A (2006) A comparison of multivariate autoregressive estimators. Signal Process 86(9):2426–2429. doi:10.1016/j.sigpro.2005.11.007
28. Hasan MK, Hossain MJ, Haque MA (2003) Parameter estimation of multichannel autoregressive processes in noise. Signal Process 83(3):603–610. doi:10.1016/S0165-1684(02)00491-7
29. Penny WD, Roberts SJ (2000) Bayesian methods for autoregressive models. In: Neural networks for signal processing X. Proceedings of the 2000 IEEE signal processing society workshop (Cat. No. 00TH8501), 2000, vol 121, pp 125–134. doi:10.1109/NNSP.2000.889369
30. Omidvarnia AH, Mesbah M, Khlif MS, Toole JMO, Colditz PB, Boashash B (2011) Kalman filter-based time-varying cortical connectivity analysis of newborn EEG. In: 2011 Annual international conference of the IEEE engineering in medicine and biology society, Aug. 30 2011–Sept. 3 2011, pp 1423–1426. doi:10.1109/IEMBS.2011.6090335

31. Giraldo E, Castellanos CG (2014) Estimation of neuronal activity and brain dynamics using a dual Kalman filter with physiologycal based linear model. Revista Ingenierías Universidad de Medellín 12(22):169–180
32. Wen P, Li Y (2006) EEG human head modelling based on heterogeneous tissue conductivity. Australas Phys Eng Sci Med 29(3):235. doi:10.1007/BF03178571
33. Bashar R, Li Y, Wen P (2008) Influence of white matter inhomogeneous anisotropy on EEG forward computing. Australas Phys Eng Sci Med 31(2):122–130. doi:10.1007/BF03178586
34. Bashar MR, Li Y, Wen P (2010) Effects of local tissue conductivity on spherical and realistic head models. Australas Phys Eng Sci Med 33(3):233–242. doi:10.1007/s13246-010-0027-3
35. Wan EA, Nelson AT (2002) Dual extended Kalman filter methods. In: Haykin S (ed) Kalman filtering and neural networks. Wiley, New York, pp 123–173. doi:10.1002/0471221546.ch5
36. Tae-Seong K, Yongxia Z, Sungheon K, Singh M (2002) EEG distributed source imaging with a realistic finite-element head model. IEEE Trans Nucl Sci 49(3):745–752. doi:10.1109/TNS.2002.1039558
37. Schimpf PH, Ramon C, Haueisen J (2002) Dipole models for the EEG and MEG. IEEE Trans Biomed Eng 49(5):409–418. doi:10.1109/10.995679
38. Pascual-Marqui RD (2002) Standardized low-resolution brain electromagnetic tomography (sLORETA): technical details. Methods Find Exp Clin Pharmacol 24(Suppl D):5–12